

Supporting Information

Electrostatic interactions *versus* van der Waals interactions in Self-assembly of Dispersed Nanodiamonds

*Qian Xu and Xiang Zhao**

Institute for Chemical Physics and Department of Chemistry, State Key Laboratory of Electrical Insulation and Power Equipment, Xi'an Jiaotong University, Xi'an 710049, China

* Corresponding Author:

Telephone number: +86-29-8266-5671

Fax number: +86-29-8266-8559

E-mail: xzhao@mail.xjtu.edu.cn

Comparison of calculation results based on universal force field and Dreiding force field

The effect of force field on the binding energy is presented in Figure 1. In the present work, two force fields are considered: universal force field and Dreiding force field. The results from both force fields indicate the same feature that the bigger the nanodiamonds are, the more stable the binding interactions are. Besides, although there is slightly energy difference in the case of C₅₄₈, the difference decreases as the size of nanodiamonds increases to C₈₃₇ and C₁₁₉₈. More

importantly, the results confirm that the first assembly property proposed in this work is not dependent on special force field, that the binding energy is as large as the dissociation energy of chemical bonds.

Figure S2 displays the relative values of total binding energy, van der Waals binding energy and electrostatic binding energy by Dreiding force field. In the graph, the average binding energy is illustrated by the horizontal line. As expected, the results demonstrate the same features as that obtained from universal force field. In detail, the ranges of total binding energy and van der Waals binding energy are almost the same, indicating van der Waals dominates the total binding energy.

Figure S3~S5 illustrate the binding energy distribution of nanodiamond C₅₄₈, C₈₃₇ and C₁₁₉₈ corresponding to various binding configurations, respectively. The results demonstrate that the relative distribution of binding energy is independent of specific force fields. Consequently, the second assembly property is independent of specific force fields that the binding interaction is directional.

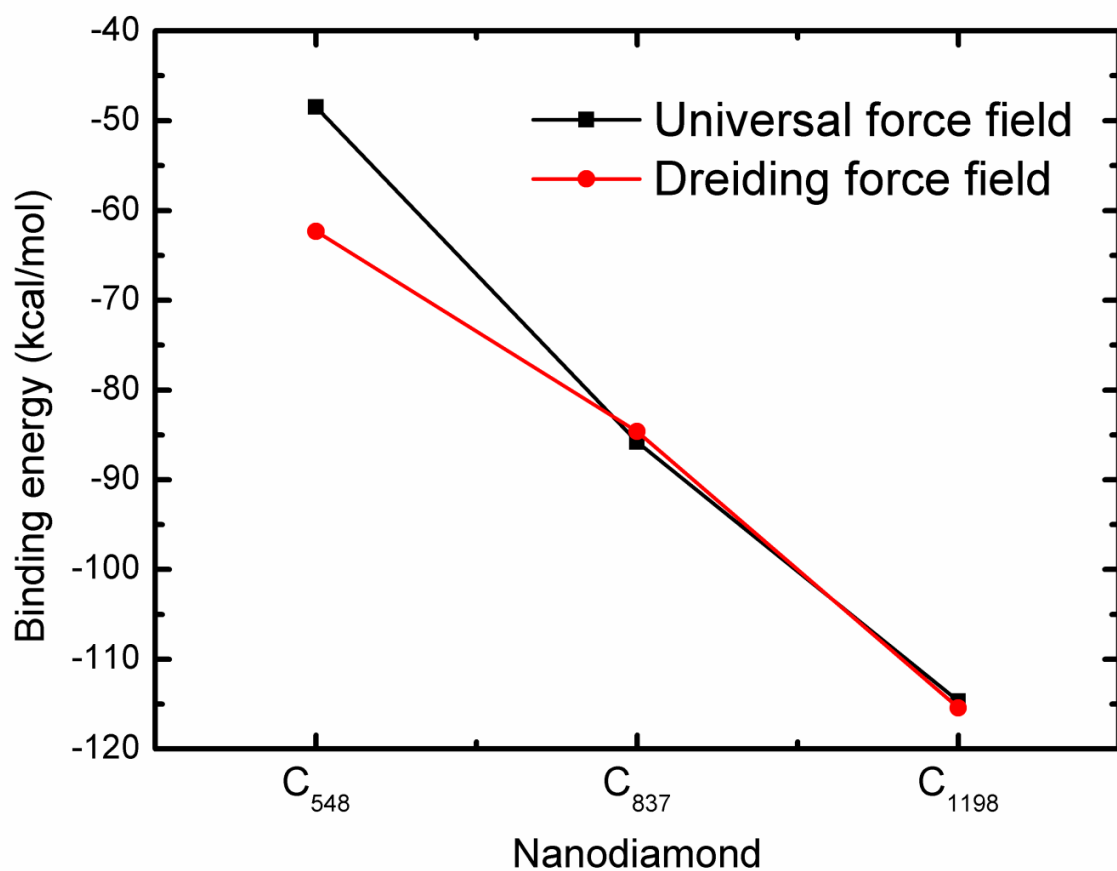


Figure S1. The binding energy of nanodiamond particles C₅₄₈, C₈₃₇ and C₁₁₉₈ calculated in both force fields.

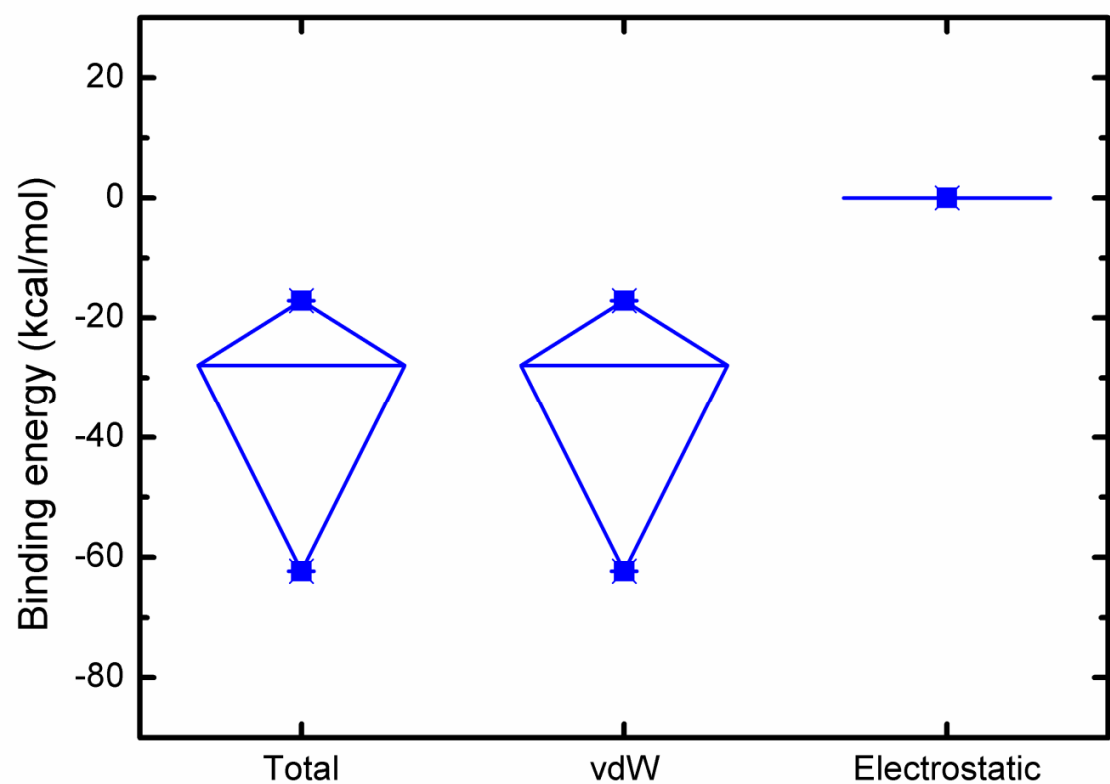


Figure S2. The contributions of van der Waals interaction and electrostatic interaction to the total binding energy of nanodiamond C₅₄₈ by Dreiding force field.

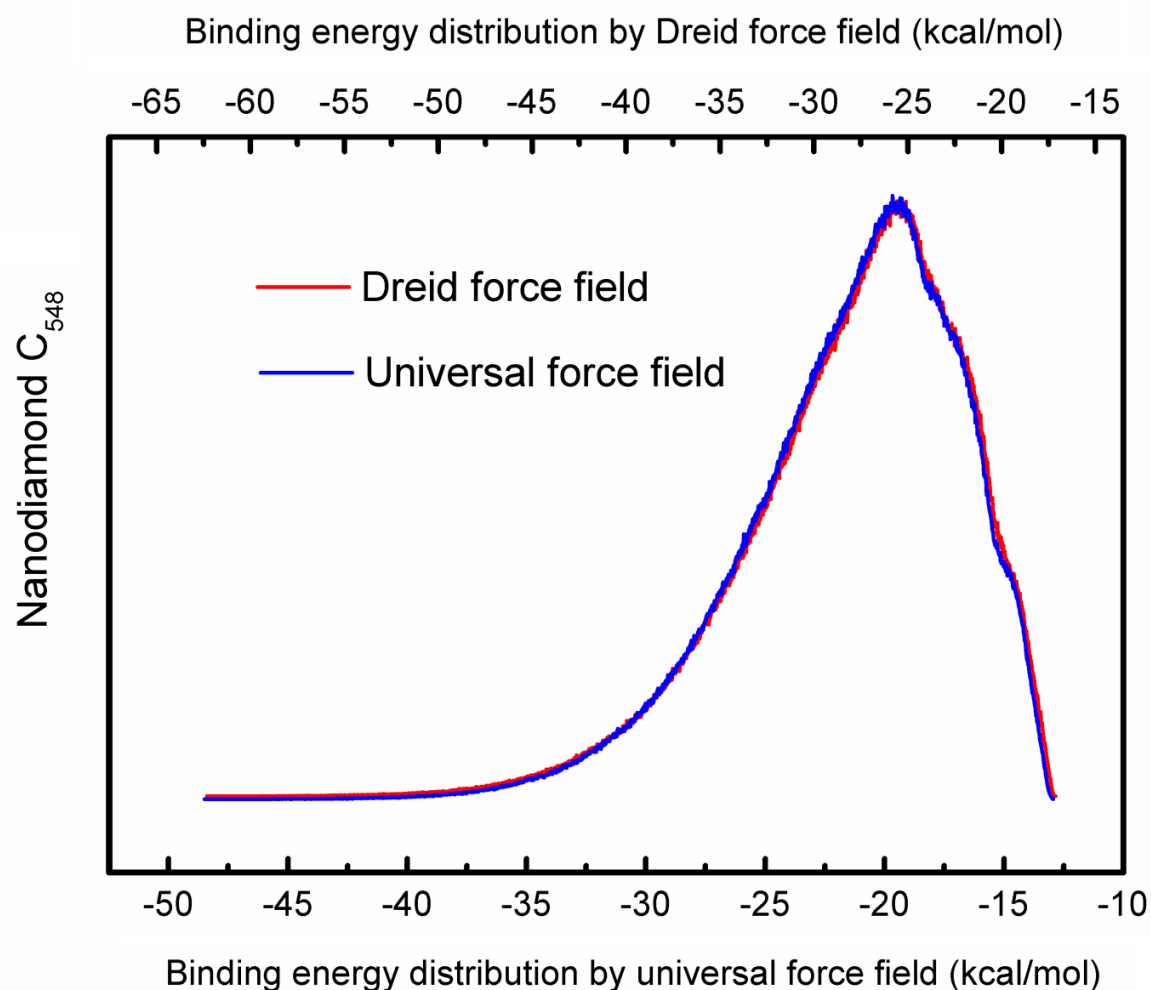


Figure S3. Binding energy distribution of nanodiamond C_{548} .

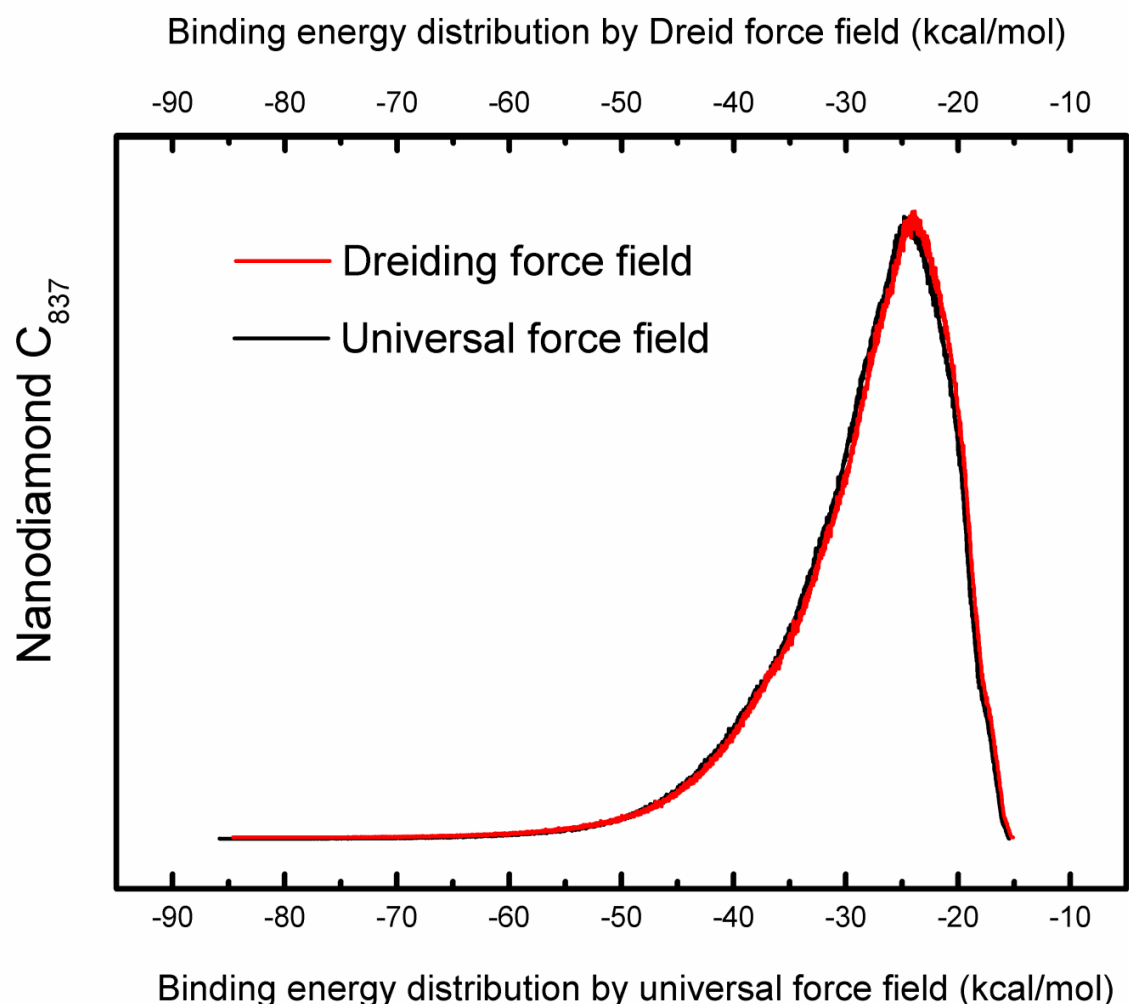


Figure S4. Binding energy distribution of nanodiamond C₈₃₇.

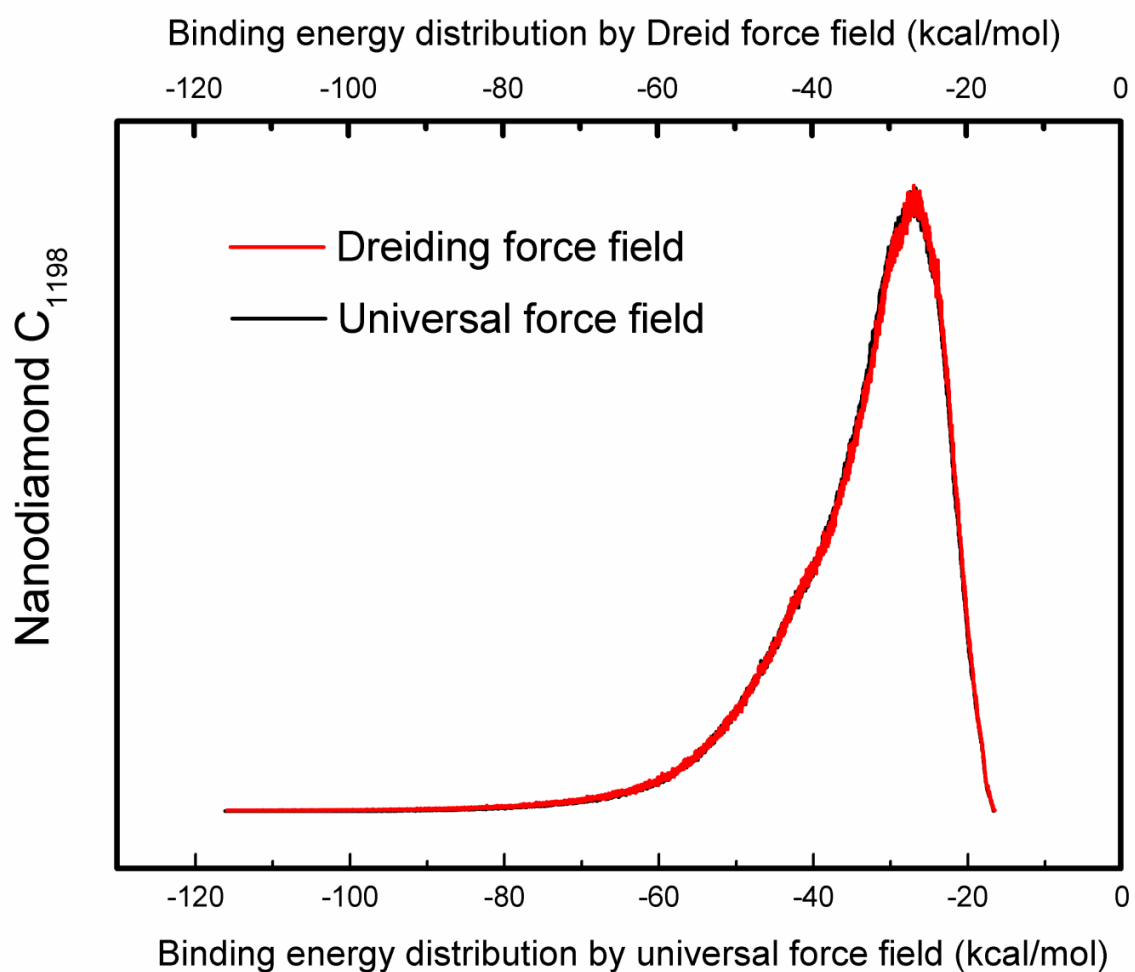


Figure S5. Binding energy distribution of nanodiamond C₁₁₉₈.

Comparison of DFT and SCC-DFTB method in calculating atomic charges of C₅₄₈

Electrostatic potential distribution is a representation of electronic properties. It is equivalent to charge density distribution based on Poisson equation. More importantly, it is a space distribution without any ambiguity. In contrast, representations of atomic charges are distinct in different computational methods as they depend on specific techniques in dividing the space charge distribution into atomic charges. In this situation, according to the relationship of electrostatic potential and atomic charges, we can distinguish the accuracy of calculated atomic

charges and whether the computational method is appropriate for the system of nanodiamond. Besides, same to fullerene, clean nanodiamond is an all-carbon system and require effective and robust methods to obtain reasonable electrostatic potential and atomic charges. In the sense, the calculated atomic charges of nanodiamond can be treated as a critical indicator in identifying the accuracy of calculation methods.

Herein, first of all, electrostatic potential of nanodiamond C₅₄₈ has been precisely calculated by all-electron *ab initio* DFT methods. In detail, it is calculated in the level of B3LYP/STO-3G and PW91/DNP, respectively, as presented in Figure S6 (a) and (c). These two potential distribution results present an overall same tendency. Especially, the (100) surfaces in both methods possess positive potential, which could be a good indicator in distinguishing the accuracy of atomic charges. Nevertheless, compared to B3LYP density functional, PW91 slightly overestimate the potential value on the (111)_S surface, leading to the areas with negative potential on the (111)_S surface is not obvious. Such variation has already been considered in the current study and will not affect the outcomes.

The Mulliken charges and NBO charges obtained in the level of B3LYP/ STO-3G are illustrated in Figure S7 (a) and (b). These two charge results are almost the same, in both sides of atomic charge distribution and range of charge value, and also agree well with the surface electrostatic potential. On the contrary, the Mulliken charges and ESP charges obtained by PW91/DNP present a totally unreasonable distribution. For example, as suggested in Figure S7 (f), (a) and (b), the atom-12 and atom-13 should take negative charges while atom-11 and atom-14 possess positive charges. But these features are not exhibited in Figure S7 (c) and (d). Moreover, for the Mulliken charges from SCC-DFTB methods as shown in Figure S7 (e), their atomic charge distribution is nearly the same with Mulliken and NBO charges by B3LYP/STO-

3G results. Nevertheless, their ranges are almost ten times larger than the results from B3LYP/STO-3G results. Because it is commonly believed that the NBO charges from *ab initio* methods are accurate, therefore, it can be conjectured that Mulliken charges by B3LYP/STO-3G are meaningful; Mulliken charges by SCC-DFTB overestimate the values; the atomic charges by PW91/DNP methods are not reasonable in the current all-carbon system.

In addition, the electrostatic potential is also calculated by semi-empirical SCC-DFTB methods in conjunction with Coulomb law, as illustrated in Figure S6 (c). Luckily, in general, such potential result agrees well with *ab initio* DFT results.

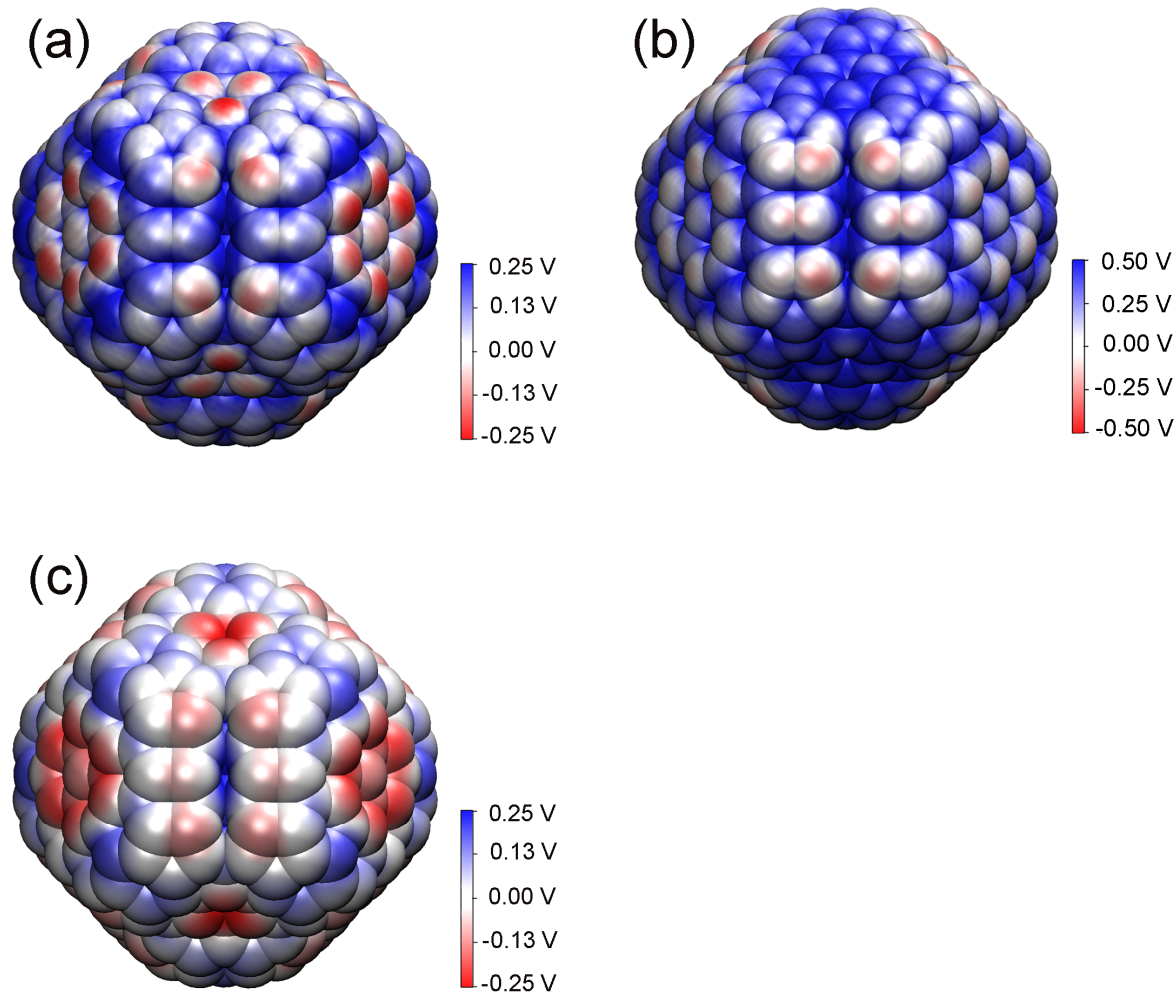


Figure S6. Electrostatic potential on the van der Waals surface of nanodiamond C₅₄₈ by (a) B3LYP/STO-3G, (b) PW91/DNP and (c) SCC-DFTB in conjunction with Coulomb law.

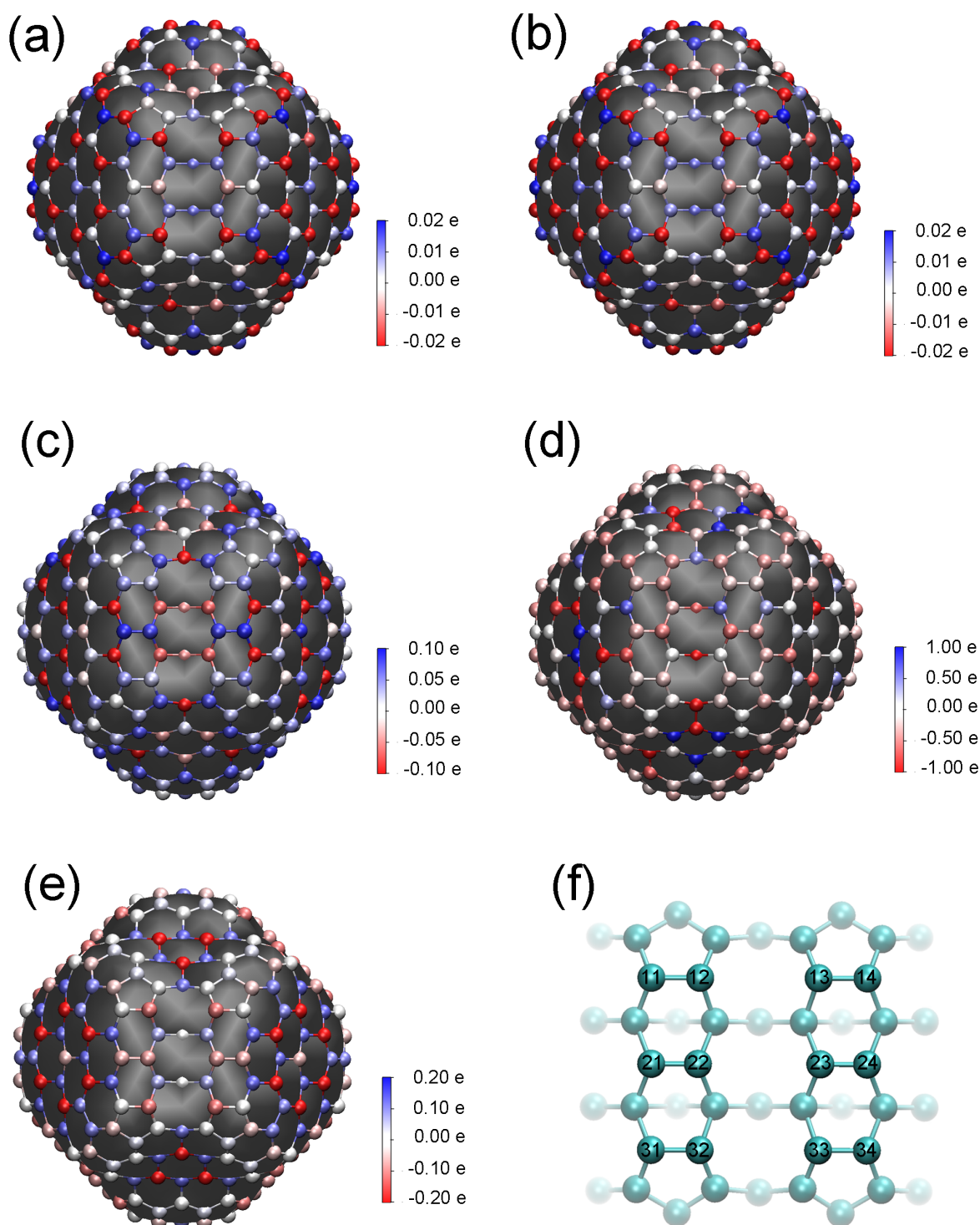


Figure S7 Atomic charge distribution by different methods: (a) Mulliken charge by B3LYP/STO-3G; (b) NBO charge by B3LYP/STO-3G; (c) Mulliken charge by PW91/DNP; (d) ESP charge by PW91/DNP; (e) Mulliken charge by SCC-DFTB; (f) atomic structure on the (100) surface.

Comparisons of the relative contribution between electrostatic interaction and van der Waals interaction for larger nanodiamonds

As discussion above, although Mulliken charges obtained from SCC-DFTB method overestimate the charge value, the charge distribution is meaningful. Herein, combined with Mulliken charges from SCC-DFTB method and Monte Carlo molecular simulations, the relative contributions of electrostatic interaction and van der Waals interaction for nanodiamond C₅₄₈, C₈₃₇ and C₁₁₉₈ are investigated. In the current additional computations, universal force field is selected and 10⁶ samples are generated for each Monte Carlo simulation.

In the text, we have already illustrated that for the case of C₅₄₈ van der Waals interactions dominates the binding energy. Here, with SCC-DFTB Mulliken charges, same conclusions are also obtained for nanodiamonds of C₅₄₈, C₈₃₇ and C₁₁₉₈, as presented in Figure S8. Although SCC-DFTB method overestimates the charge values, the electrostatic interactions are still much smaller than the van der Waals interactions in these systems.

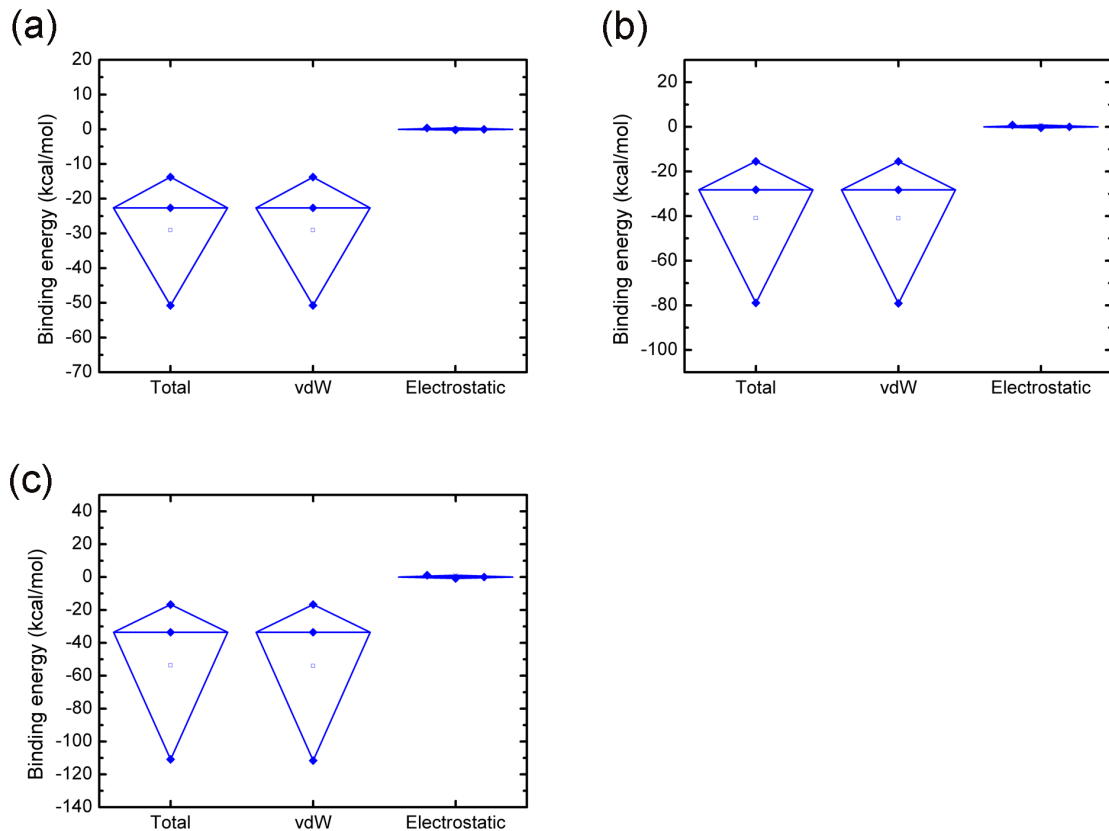


Figure S8 ranges of total, van der Waals and electrostatic interaction energies of nanodiamond (a) C₅₄₈, (b) C₈₃₇ and (c) C₁₁₉₈, the horizontal lines indicate the average binding energies, and the range of electrostatic interaction energy is so small that the upper limit and lower limit almost overlap.